Journal of Alloys and Compounds 663 (2016) 123–127

Contents lists available at ScienceDirect

Journal of Alloys and Compounds

journal homepage: http://www.elsevier.com/locate/jalcom

First-principles study of electronic, thermoelectric and thermal properties of Sb_2S_3

T. Ben Nasr [a, *], H. Maghraoui-Meherzi [b], N. Kamoun-Turki [a]

[a] Laboratoire de Physique de la Matière Condensée, Département de Physique, Faculté des Sciences, Université Tunis El-Manar, Tunis 2092, Tunisia
[b] Laboratoire de Chimie Analytique et d'Electrochimie, Département de Chimie, Faculté des Sciences, Université Tunis El-Manar, 2092, Tunisia

ARTICLE INFO

Article history:
Received 31 July 2015
Received in revised form
9 November 2015
Accepted 13 December 2015
Available online 15 December 2015

Keywords:
Ab-initio calculation
Electronic structure
Thermoelectric properties
Thermal properties

ABSTRACT

A theoretical study of the electronic, thermoelectric and thermal properties of Sb_2S_3 is presented using the full potential linearized augmented plane wave (FP-LAPW) method within density functional theory (DFT). In this approach, the modified Becke Johnson (TB-mBJ) potential was used for the exchange-correlation potential calculation. Our calculations indicate that Sb_2S_3 exhibit direct band gap, if we exclude some indirect transitions marginally below the direct gap. The obtained band gap of 1.88 eV is in agreement with the experimental values as compared to other calculations. The electron and hole effective mass for Sb_2S_3 is analysed in detail. The electronic transport properties are obtained via Botzmann transport theory. The predicted Seebeck coefficient is 2888 μV/K and the thermoelectric performance can be optimized by n-type doping at room temperature. Moreover, employing the quasi-harmonic Debye model as implemented in Gibbs code, the thermal properties were evaluated.

1. Introduction

Antimony sulfide (Sb_2S_3) is an important semiconducting chalcogenide member of the V-VI main group compounds. It is widely used in thermoelectric cooling devices, solar energy conversion and optoelectronics in IR region. Sb_2S_3 has a band gap that is varied between 1.5 and 2.2 eV by changing the size, shape, and crystallinity in the nanoscale regime [1]. Sb_2S_3 is an important photoconductive semiconductor that crystallizes in the orthorhombic system with the Pnma space group (No. 62) [2]. There is also a surge of interest in using Sb_2S_3 as a solid-state semiconductor-sensitized solar cell to replace the inorganic dye in dye-sensitized solar cells [3,4]. Sb_2S_3 has been synthesized in various nanostructured forms, such as nanowires and nanotubes, which exhibit enhanced ferroelectric, piezoelectric, and conductive properties [5–7]. So far, much focus has been placed on the synthesis and electronic properties [8–11] of Sb_2S_3. To complement these known aspects, we present here a study of the electronic, thermoelectric and thermal properties of Sb_2S_3 using density-functional theory (DFT). To the best of our knowledge, there are no theoretical works exploring the thermoelectric and thermal properties. Our calculation show that the n-type doped Sb_2S_3 is a promising thermoelectric material. Moreover, the effective mass of Sb_2S_3 is discussed in detail to understand the physical mechanism of its thermoelectric property. Finally, the quasi-harmonic Debye model was successfully used to determine the thermal properties.

2. Computational details

The calculations were performed by using the full-potential linearized augmented plane-wave (FP-LAPW) method as implemented in WIEN2K package. The exchange-correlation functional was described by Generalized Gradient Approximation (GGA) [12] for structural relaxation, while the Tran-Blaha modified Becke-Johnson (TB-mBJ) approximation [13] was used for electronic structure properties. The plane wave cutoff parameter $R_{MT}K_{max} = 6$ where R_{MT} is the minimum radius of the muffin-tin spheres and K_{max} represents the magnitude of the largest k-vector in the plane wave expansion. In order to avoid the overlapping the atomic sphere radii are chosen as small as possible ($R_{MT} = 2.4$ a.u for Sb and $R_{MT} = 2.0$ a.u for S). The maximum value of angular momentum (l_{max}) is set to be 10 for the spherical harmonics expansion inside the muffin-tin spheres while the Fourier expansion of charge density was setup at $G_{max} = 12$ which ultimately correspond to a good compromise between computational time and accuracy. The Brillouin zone integrations were performed using 2000 k-points.

* Corresponding author.
E-mail address: tarek.ben-nasr@laposte.net (T. Ben Nasr).

http://dx.doi.org/10.1016/j.jallcom.2015.12.093
0925-8388/

We used a self-consistent criterion of the total energy with a precision of 10^4 Ry. The investigations of thermoelectric properties in this study were done within the semi-classical Boltzmann theory, as implemented in BoltzTraP code [14], which has proven to be one of the most theory for the computation of the lattice dynamics of crystals. Thermal properties were investigated using the quasi-harmonic Debye model implemented in the Gibbs program [15] to determine all the thermodynamic parameters as a function of temperature and pressure.

3. Results and discussion

3.1. Band structure

A comparison of the theoretical studies published so far shows some inconsistencies in the calculated band gap, the values reported for stibnite are in the range 1.18–1.76 eV [9,16,17]. In addition Sb_2S_3 exhibit closely lying direct and indirect transitions, thereby complicating the assignment of the nature of the gap. For instance, in a previous work we report a direct gap of 1.76 eV [8], while J.J. Carey et al. [18] gave an indirect gap of 1.29 eV. Within this context we perform a calculation of the band structure with a denser set of k-points. Fig. 1 shows the TB-mBJ band structure of Sb_2S_3 along the principal high-symmetry directions in the Brillouin zone. Several extrema were revealed in proximity of the fundamental gap, making the direct and indirect transitions almost degenerate. Table 1 shows that the energy separation between direct and indirect band gap falls within 0.15 eV. The data in the table suggest that in this case the direct transition will most likely dominate over the indirect one, apart from a very narrow onset of 0.1–0.2 eV [10]. This observation is consistent with experimental evidence showing a weak absorption onset just below the threshold for direct absorption [19,20]. Furthermore, the band gap

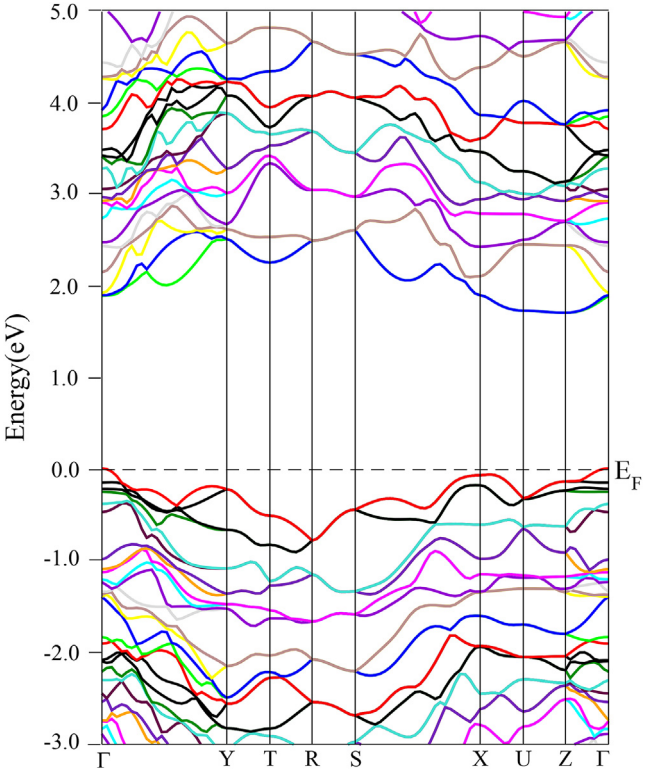

Fig. 1. Band Structure of Sb_2S_3.

Table 1
Comparison between the minimum band gap and the direct band gap of Sb_2S_3 as obtained from TB-mBJ calculation. All values are in units of eV.

	Minimum gap	Direct gap
Sb_2S_3	1.73	1.88

of stibnite has been measured extensively via optical absorption experiments. Almost, all reported a direct band gap between 1.42 and 1.88 eV [1,21,22]. These results suggest that Sb_2S_3 can be considered direct gap semiconductor. The calculated direct gap for the Γ point is 1.88 eV. Compared to the experimentally reported values the calculated gap is in closer agreement. However, the TB-mBJ gap is larger than a previous local density approximation (LDA) calculations reporting a gap of 1.55 eV [9] and the GGA calculations which found a gap of 1.18 eV [16]. This is an expected result since both LDA and GGA underestimate the energy gap [23].

3.2. Effective mass

To provide a link between band structure and transport properties, the effective mass tensor for electrons and holes using the band structure data obtained was calculated. The hole masses along the principal axes of the ellipsoidal energy surface were calculated at the valence band maximum while the electron masses were calculated at the conduction band minimum. The principal axes were chosen along the reciprocal lattice vectors of the orthorhombic brillouin zone. We estimated these two effective masses through a simple parabolic fitting using the definition of effective mass as a second derivative of energy band with respect to the wave vector, k:

$$\frac{1}{m^*} = \frac{\partial^2 E(k)}{\hbar^2 \partial k^2}, \tag{1}$$

The results are shown in Table 2, unfortunately, we cannot find the corresponding experimental data for comparison. As it is seen the effective mass of electron at the conduction band minimum is smaller than that of the holes at the valence band maximum. Consequently, Sb_2S_3 should be an n-type semiconductor, consistent with the experimental result [24–26]. The average effective mass of electron in Sb_2S_3 is 0.536 m_0 whereas the effective mass of hole is 0.687 m_0. However, the electron effective mass shows a typical anisotropy and along b axis it is 1.062 m_0, but along ac plane it is lighter. These results indicate that its electrical conductivity perpendicular to b axis is much higher than that parallel to the b axis in Sb_2S_3 [27]. The electrical conductivity property of Sb_2S_3, which has a free carrier gas along ac plane and a potential barrier along b axis, could improve the Seebeck coefficient according to Hicks model [28].

3.3. Thermoelectric properties

The electronic conductivity and Seebeck coefficient tensors as a function of temperature T and the chemical potential μ can be written as [29]:

Table 2
The effective masses along the principle axes for valence and conduction band states at the Γ point in the units of the free-electron mass in the vicinity of the gap.

Band no.	Energy (eV)	m_a	m_b	m_c	Average
96	4.251	0.901	0.435	0.725	0.687
Gap	–	–	–	–	–
97	5.980	0.382	1.062	0.164	0.536